Electrical Interconnects Fabricated From Biodegradable Conductive Polymer Composites

Tao Zhang, Melissa Tsang, *Student Member, IEEE*, Lin Du, Minsoo Kim, and Mark G. Allen, *Fellow, IEEE*

***Abstract*— This paper presents the development and characterization of biodegradable electrical interconnects for transient implantable medical devices. The interconnects comprised micropatterned biodegradable conductive polymer composites, which were developed using iron (Fe) microparticles as the conductive filler and polycaprolactone (PCL) as the insulating matrix. The electrical properties of the composites were investigated under various degradation conditions. Electrical percolation was observed at 17% Fe volume fraction, but higher volume fractions exhibited more stable electrical resistivity throughout the time course of physiological degradation. The electrical resistivity of 40%vf Fe-PCL composites increased tenfold in an emulated packaged environment under degradation. Biodegradable electrical interconnects based on 40%vf Fe-PCL composites were successfully micropatterned in daisy-chain structures, illustrating the process compatibility of Fe-PCL composites for interconnect applications. The electrical resistance of the packaged daisy-chain structures exhibited a reasonable increase under degradation. An electrical lifetime of over five days was also achieved. System integration with a commercial humidity sensor and analytical calculations supporting other application scenarios confirmed the feasibility of micropatterned Fe-PCL interconnects for use in implantable electrical systems.**

***Index Terms*— Biodegradable electrical interconnects, daisy-chain structure, Fe-PCL composite, screen printing, system integration.**

I. Introduction

IMPLANTABLE medical devices can facilitate medical treatment in multiple scenarios, such as providing *in situ* measurements of relevant physiological metrics (e.g., oxygen tension, pH, and temperature) [1]. Biodegradable medical devices, which can gradually decompose and be expelled from the body, may be useful for the monitoring of transient conditions. In such scenarios, patients do not need a second surgery to remove the devices from their bodies after the device is no longer needed [2]–[4]. In addition, biodegradable devices have the potential to overcome the negative effects associated with permanent implants, such as fibrous encapsulation and stress-shielding at the implant–tissue interface. For these reasons, biodegradable implantable devices have been proposed for the monitoring and treatment of short-term ailments [5]. Biodegradable analogues of passive RF pressure sensors have previously been demonstrated, where degradation lifetime can be tailored based on the material composition and sensor design. For example, the degradation rate of zinc (Zn)/iron (Fe) inductors used in sensors can be controlled by altering the exposed area ratio of the two metals [3], [6]. To date, biodegradable devices have been limited to either passive designs or active devices with short (i.e., minutes to hours) functional lifetimes [7]. To achieve active biodegradable devices with clinically relevant functional lifetimes, research must address not only the sensor and power source [8] but also the circuitry and electrical interconnects.

Nondegradable polymer–metal composites have been studied previously for use as electrical interconnect materials in electronic packaging. Conductive composite materials provide many advantages compared to traditional interconnect technology, such as low-temperature processing conditions that support the use of heat-sensitive and inexpensive components and substrates, less-hazardous environmental waste, lower cost processing, reduced stress on the substrates, and the ability to pattern fine-pitch interconnects, facilitating the miniaturization of electronic systems [9]. Generally, these interconnect materials are developed using metal (e.g., silver, gold, and nickel) as the conductive filler and polymer (e.g., epoxy, silicone, and polyimide) as the insulating matrix [9]. With appropriate materials modification, conductive polymer composites present an interesting avenue for biodegradable system interconnects.

To develop biodegradable electrical interconnects featuring polymer–metal composites, biodegradable polymers and metals need to be implemented. Clinically approved biodegradable polymers typically decompose into small molecules that are involved in metabolic pathways or removed from the body through natural pathways [10]. Biodegradable polymers can be categorized into two types of polymers. One type is hydrolytically degradable polymers (i.e., featuring unstable

Manuscript received August 20, 2018; revised February 4, 2019; accepted March 11, 2019. Date of publication March 14, 2019; date of current version May 7, 2019. This work was supported in part by the National Institute of Health under Grant R21-AR066322, in part by the National Science Foundation under Grant CMMI-1362652, and in part by the NSF National Nanotechnology Coordinated Infrastructure Program under Grant 15-42153. Recommended for publication by Associate Editor A. Jain upon evaluation of reviewers' comments. (*Corresponding author*: *Tao Zhang.)*

T. Zhang, L. Du, M. Kim, and M. G. Allen are with the Department of Electrical and Systems Engineering, University of Pennsylvania, Philadelphia, PA 19104 USA (e-mail: taozhan@seas.upenn.edu; dulin@seas.upenn.edu; minsook@seas.upenn.edu; mallen@seas.upenn.edu).

M. Tsang was with the School of Electrical and Computer Engineering, Georgia Institute of Technology, Atlanta, GA 30332 USA (e-mail: melissa.x.tsang@gmail.com).

Color versions of one or more of the figures in this paper are available online at http://ieeexplore.ieee.org.

Digital Object Identifier 10.1109/TCPMT.2019.2905154

chemical bonds in the polymer backbone susceptible to hydrolysis), such as poly(α-esters) and polyurethanes. The other type is enzymatically degradable polymers, such as proteins and collagen [11]. Polyesters [e.g., polycaprolactone (PCL), poly(lactic acid) (PLA)] have been particularly appealing for implants because they can be easily degraded by the hydrolysis of the ester linkage, their degradation products can be resorbed through metabolic pathways, and their structure can be modified to alter degradation rates [12]. Biodegradable metals include magnesium (Mg), Zn, Fe, and their alloys that are widely used for orthopedic and stents application [13], [14].

The behavior of such composite interconnects can be studied by the use of percolation theory. The percolation theory is a statistical model that describes how randomly positioned sites are connected in a disordered system. Above a critical concentration of positioned sites, or the percolation threshold, a connected path is formed through the system [15]. The percolation theory has been used to interpret the electrical percolation of composite materials consisting of conductive filler in an insulating matrix. Composites behave as insulators and as conductors when the concentration of conductive filler is far below and above the percolation threshold, respectively. Furthermore, composites show an appreciable change in electrical resistivity when the concentration crosses the percolation threshold [16].

We present the development of electrical interconnects comprising biodegradable conductive polymer composites for use in transient implantable systems. The electrical and mechanical properties of the composites were investigated during physiological degradation. The percolation threshold of the composites was identified. Compositions featuring reasonably stable properties were selected for subsequent testing. The electrical properties of select compositions were investigated in constructs representative of biodegradable packaging during degradation. Biodegradable electrical interconnects were micropatterned to demonstrate their compatibility with microelectromechanical system (MEMS) processing. In addition, the electrical properties of packaged interconnects were investigated during degradation to demonstrate their potential application as biodegradable interconnect materials. Finally, system integration with commercial electronic components was performed to illustrate the possibility of these composites for use in electrical systems.

II. Fabrication

A. Biodegradable Conductive Polymer Composites

Biodegradable conductive polymer composites were developed using Fe microparticles as the conductive filler and PCL as the insulating matrix. Iron was chosen for its relatively low degradation rate, compared to other biodegradable metals (e.g., Mg and Zn) [17]–[19]. In turn, PCL was selected due to its slow degradation rate and high processability [11]. To fabricate the conductive polymer composites, Fe powder (diameter <10 μm, $\geq$99.9% trace, Sigma Aldrich) was serially washed with dichloromethane ($\geq$99.8%, Sigma Aldrich) and 1,4-dioxane (99.5%, Acros Organics) in triplicate. PCL (average M_n 80 000, Sigma Aldrich) pellets were solubilized in dioxane to a concentration of 200 mg/mL. Oleic acid (90%, Sigma Aldrich) was then added to the serially washed Fe as a surfactant to facilitate the homogeneous suspension of Fe in the PCL solution. Oleic acid was selected because it is a commonly used surfactant to stabilize magnetic nanoparticles and its biocompatibility has been demonstrated [20], [21]. Finally, the PCL solution was added to the Fe/oleic acid mixture to reach the desired volume fraction.

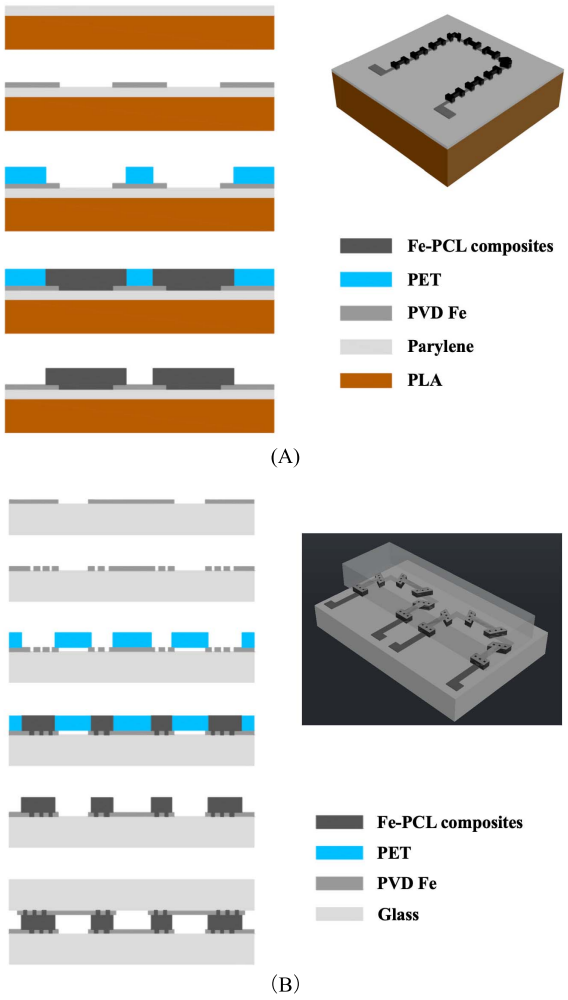

Fig. 1. Fabrication scheme and daisy-chain structures of Fe-PCL biodegradable electrical interconnects. (a) In-plane structure. (b) Out-of-plane structure.

B. Biodegradable Daisy-Chain Structures

Two types of daisy-chain structures (i.e., in-plane and out-of-plane) were developed to demonstrate that the composites can be used as interconnect materials bridging discrete electronic components in the same layer and between different layers, respectively (see Fig. 1). For the in-plane structure, 4-μm-thick parylene was first deposited on a commercial PLA substrate (2.5-mm-thick, small parts) with an SCS PDS2010 Parylene Coater. The parylene served as an insulation layer to prevent the underlying PLA substrate from being solubilized by the 1,4-dioxane in the composite solution to facilitate composite characterization and would be omitted in an actual biodegradable implant fabrication. The substrate

was then metallized with Fe traces 100 nm in thickness by sputter deposition through a shadow mask to simulate discrete electronic components in the same layer. Next, screen printing of the composite was performed using 10-mil-thick polyester shim micromachined with a CO_2 laser as the stencil. The patterned shim was then applied onto the PLA substrate, after which the Fe-PCL composite (40%vf of Fe) was screen printed onto the substrate. For the out-of-plane structure, glass substrates were used for more convenient alignment in the final step, but can be modularly replaced with biodegradable substrates. First, Fe traces 100 nm in thickness were sputter deposited onto a glass substrate through a shadow mask and patterned by laser micromachining (532 nm wavelength, 100 μJ pulse energy, 1 ns pulsewidth, and 10 W maximum power) to simulate discrete electronic components on one layer. Specifically, 25% of the Fe surface area of each pad was ablated to expose the underlying glass to promote adhesion of the composites. Next, the Fe-PCL composite (40%vf of Fe) was screen printed through a patterned shim onto the prepatterned Fe-glass substrate. In the same manner, composites were screen printed onto a second glass substrate with a complementary pattern of sputter-deposited 100-nm-thick Fe traces to represent the second layer. Finally, two glass substrates were flip-bonded at 82 °C and 202 kPa with a heat press for 5 min. In this manner, in-plane and out-of-plane electrically continuous daisy-chain structures were formed.

C. Packaging

In actual application, medical devices are packaged so electrical interconnects will not be directly exposed to the body fluid after implantation. In order to emulate this situation, packaging of the daisy-chain structure with encapsulating PCL film was performed. First, PCL pellets were heat pressed into a 150-μm-thick film at 82 °C and 3040 kPa for 30 min and cut to a square size of 10 cm × 10 cm. Wires were soldered to both ends of the daisy-chain structure for future resistance measurement. The PCL square film was folded in half, and the sample bearing daisy-chain structures with soldered wires was placed inside. The edges of the folded film were melt-joined on a PDMS substrate at 70 °C, so the folded film became a sealed biodegradable package.

III. Characterization

A. Composites in Physiological Degradation

1) Electrical Properties: As electrical conductivity is a key design requirement for interconnects, the effect of physiological degradation on the electrical resistivity of Fe-PCL composites was investigated. Composite films with different volume fractions of Fe were prepared and immersed in simulated body fluid (SBF) at 37 °C in an incubator to simulate physiological degradation. At intermittent time points, the resistivity of the films was measured using electrical probe testing.

Fig. 2 shows the electrical resistivity of Fe-PCL composite films as a function of volume fraction, parameterized by the duration of physiological degradation. Except for one outlier at 6 h and approximately 17%vf, potentially attributable to a systemic measurement error, the electrical resistivity of all preparations decreased by orders of magnitude between 10% and 20% volume fractions of Fe with a percolation threshold at approximately 17%vf, above which the electrical resistivity did not appreciably change. However, the resistivity of the composites with a higher volume fraction of Fe (i.e., $\geq$40%) exhibited enhanced stability. A potential explanation is that with physiological degradation, Fe corrosion products, such as oxides formed, present an electrical barrier to conduction, thus a smaller percentage of Fe was transformed to oxides in composites with higher volume fraction of Fe as degradation proceeds (since the initial amount of Fe at higher volume fractions is higher). As electrical stability over time of the interconnect is an important parameter, composites with 40%vf of Fe were selected for use in subsequent testing.

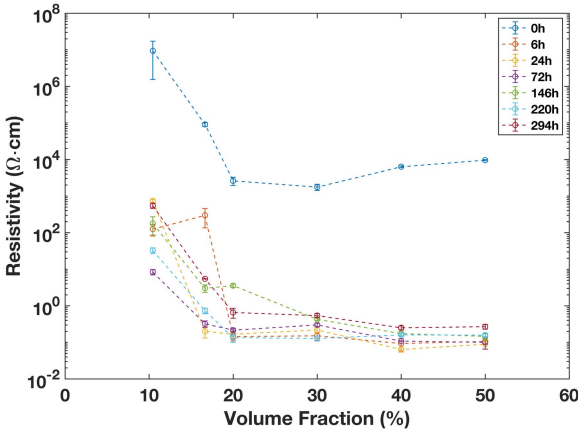

Fig. 2. Electrical resistivity of Fe-PCL biodegradable conductive polymer composite films at varying volume fractions of Fe, parameterized by degradation time.

2) Mechanical Properties: The functional lifetime of electrical interconnects may also be limited by adhesion strength. Since physiological degradation may further exacerbate the effect, it was important to enhance the adhesion strength of Fe-PCL composites on biodegradable substrates and to ensure that the adhesion persists throughout physiological degradation. Toward these goals, as well as to demonstrate the processing compatibility of biodegradable Fe-PCL interconnects on similarly biodegradable substrates, Fe-PCL electrical interconnects were screen printed onto micropatterned Fe-PLA substrates. Specifically, Fe traces were micropatterned onto a 250-μm-thick PLA substrate by sputter deposition through a shadow mask to form a grid of 10 mm × 10 mm squares of 100 nm thickness. Next, the sputtered Fe was ablated with an array of 250-μm-wide square holes to expose 25% of the underlying PLA and Fe-PCL composite (40%vf of Fe) was screen printed onto the micropatterned Fe using the fabrication procedure described earlier. Note that this approach allowed Fe-PCL composite material to be in contact with the PLA substrate through the ablated hole array in the Fe pads. Samples were then diced into individual coupons comprising three test samples per coupon and immersed in SBF at 37 °C for physiological conditioning.

At periodic time points, samples were retrieved for optical microscopy and adhesion testing in accordance with ASTM D3359-09 guidelines [22]. Briefly, two intersecting cuts were made through the Fe-PCL composite in each sample using

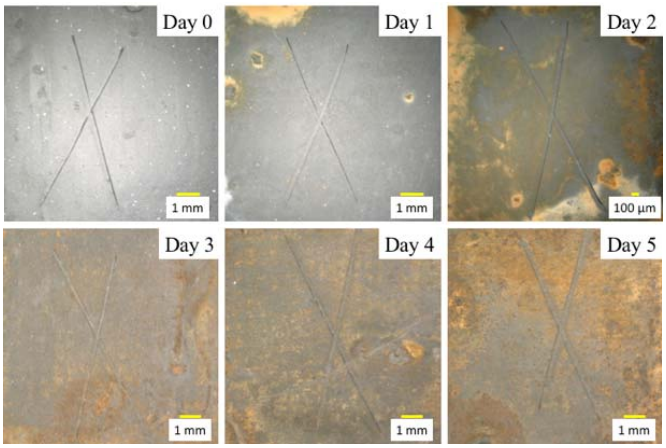

Fig. 3. Optical images of physiologically conditioned Fe-PCL composites (40%vf of Fe) after adhesion tests were performed on PLA substrates with micropatterned Fe traces.

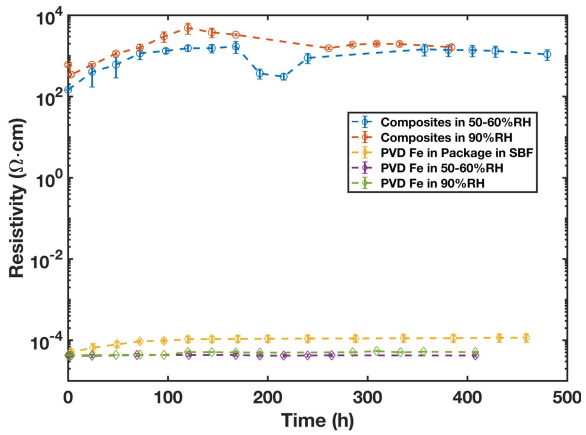

Fig. 4. Electrical resistivity of Fe-PCL biodegradable conductive polymer composite films (40%vf of Fe) and sputter-deposited Fe traces as a function of degradation time under various conditions.

a razor blade; the intersection point was aligned with the center of each square pattern and the intersection angle ranged between 30° and 45°. For each test, a 75-mm-long strip of Scotch permanent tape was adhered onto the cut Fe-PCL composite with the tape running in the same direction as the smaller intersecting angle. Good contact was ensured before proceeding. Within 90 ± 30 s of application, the tape was pulled off rapidly at a peel angle as close to 180° as possible. Finally, the cut area was inspected for the removal of composites from the substrate, and adhesion was rated based on the ASTM scale. The scale ranges from 0 to 5, which corresponds to the complete removal of the adhesive material (i.e., poorest adhesion) and negligible loss of adhesive material, respectively.

As biodegradable electrical interconnects must maintain adhesion onto similarly biodegradable substrates, the adhesion of Fe-PCL composites on Fe-PLA substrates was investigated with respect to degradation time (see Fig. 3). From previous experiments, it was found that the composites showed poor adhesion on stainless steel substrates, where composites could be peeled off without effort (i.e., a rating of 0 in adhesion tests). Furthermore, it was hypothesized that the corrosion products formed during degradation could embrittle the Fe-PCL composite and deteriorate its adhesion. However, the design of the Fe traces presented in this paper, which featured 25% areal exposure of the underlying PLA substrate, demonstrated significantly improved adhesion with Fe-PCL composite. Specifically, the composites scored the maximum adhesion rating (i.e., 5) and retained their adhesion strength throughout the time course of degradation. The results not only confirmed that the design of the micropatterned Fe traces and Fe-PCL composite can successfully resolve previous adhesion challenges, but also support their use for biodegradable electrical interconnects in transient implantable applications.

B. Electrical Properties of Composites in Emulated Packaged Environment in Degradation

Since the composites will be used as interconnect materials in a biodegradable packaged system, it is essential to characterize the electrical properties of the composites in a similar environment. In a PCL-packaged system exposed to SBF, the electrolyte can permeate the PCL film and react with the composites; thus, a humid condition is a potential simulation to the packaged environment. Two conditions with significantly different humidity values were utilized for the conditioning studies. In the first condition, composite films were placed next to a beaker full of distilled water in a covered container at 37 °C in an incubator. The relative humidity (RH) measured inside the container was between 50% and 60%. In the second condition, composite films fixed onto a glass slide were flipped so that the exposed composite surface faced downward above a container of distilled water. The sample was maintained at 37 °C in an incubator. The RH measured inside the container was 90%. Composite films with 40%vf Fe and physical vapor deposition (PVD) Fe traces (100 nm thickness) were prepared and exposed to these two conditions. At periodic time points, the resistivity of the films and Fe traces was measured using electrical probe testing.

Fig. 4 shows the electrical resistivity of 40%vf Fe-PCL biodegradable conductive polymer composite films and sputter-deposited Fe traces (100 nm thickness) as a function of degradation time for various degradation conditions. The resistivity of the composite films increased at the beginning of the degradation test and continued to increase by approximately tenfold over 200 h in both humid conditions. This may be attributed to iron oxidation in the presence of moisture, which marked a stark difference from composites immersed in SBF. Specifically, samples exposed to SBF showed a significant initial reduction in resistivity due to electrolyte permeation of the bulk PCL matrix (shown in Fig. 2). The resistivity of composite films increased at a similar rate in both humid conditions, supporting the speculation that the composite degradation mechanisms under the two conditions were similar. An inflection point was observed between 100 and 200 h in both curves, which may be attributed to the formation of hydrated iron oxide. This provides mobile ions that increase the conductivity of composites [23]. The resistivity of the sputter-deposited Fe traces remained low in both humid conditions for over 400 h, similar to the

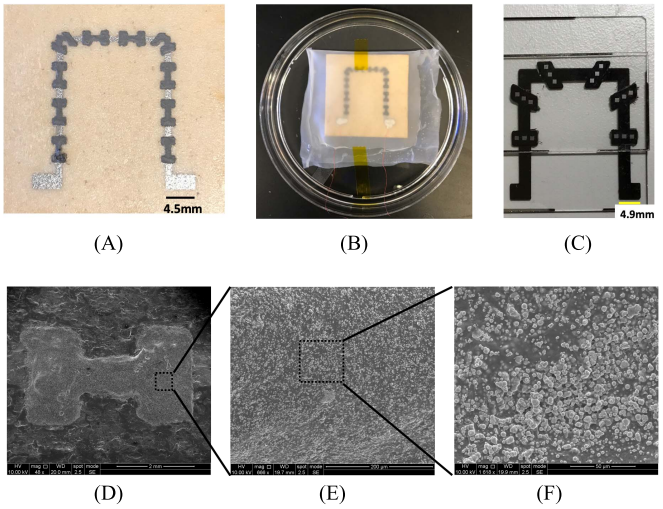

Fig. 5. Optical and SEM images of micropatterned biodegradable daisy-chain structures comprising Fe-PCL conductive polymer composites as interconnects bridging sputter-deposited Fe traces. Optical images of (a) in-plane structure, (b) in-plane structure packaged in PCL and exposed to SBF, and (c) out-of-plane structure. (d) In-plane structure under SEM (48× magnification), (e) higher magnification (666×) of the black dotted box in (d), and (f) higher magnification (1618×) of the black dotted box in (e).

resistivity of the packaged Fe traces under physiological degradation.

C. Optical Images of Daisy-Chain Structures

Fig. 5 shows the micropatterned biodegradable daisy-chain structures comprising Fe-PCL conductive polymer composites as interconnects bridging sputter-deposited Fe traces. In the in-plane structure [see Fig. 5(a)], the interconnect width and thickness were approximately 600 and 200 μm, respectively, which support the dimensions of typical MEMS interconnection [24]. Together, the daisy-chain structures demonstrate the feasibility of interconnect patterning using Fe-PCL composites with standard MEMS processing techniques. Fig. 5(b) shows a sample bearing in-plane daisy-chain structures encapsulated in PCL and exposed to SBF, simulating interconnects with biodegradable packaging in physiological degradation. In the out-of-plane structure [see Fig. 5(b)], the laser-machined Fe traces featuring 25% areal exposure of the underlying glass substrate can be observed. Glass in the ablated regions is in direct contact with the overlying screen-printed Fe-PCL composite to promote adhesion. The SEM image [see Fig. 5(d)] shows the surface morphology of the daisy-chain structures, and zoomed-in images [see Fig. 5(e) and (f)] show the size of the Fe microparticles (<10 μm).

D. Electrical Properties of Daisy-Chain Structures in Biodegradable Package in Degradation

In order to investigate the performance of Fe-PCL interconnects with representative packaging and conditioning, the electrical resistance of daisy-chain structures packaged in PCL was measured throughout degradation. For these studies, degradation was simulated by immersion in SBF at 37 °C. Packaged daisy-chain structures and packaged sputter-deposited Fe traces

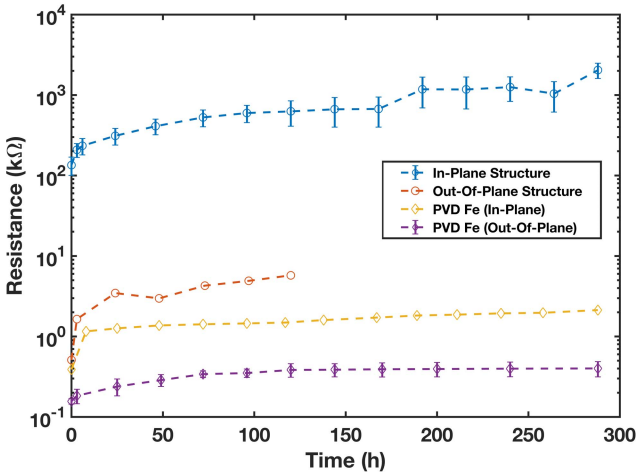

Fig. 6. Electrical resistance of packaged biodegradable daisy-chain structures and packaged sputter-deposited Fe traces as a function of degradation time.

(100 nm thickness) featuring the same lateral dimensions were prepared and immersed in SBF at 37 °C in an incubator. At intermittent time points, the resistance of the daisy-chain structures and Fe traces was measured using a multimeter.

Fig. 6 shows the electrical resistance of daisy-chain structures and sputter-deposited Fe traces in PCL packaging as a function of degradation time. PVD Fe (in-plane structure) and PVD Fe (out-of-plane structure) have the same geometries as the in-plane and out-of-plane daisy-chain structures, respectively. Calculated by the dimensions of the daisy-chain structures, the resistance of the in-plane structure was approximately 200 kΩ and the resistance of the out-of-plane structure was approximately 400 Ω, both of which were consistent with the measured resistance before degradation. The resistance of in-plane and out-of-plane daisy-chain structures increased as degradation proceeded and electrical lifetimes over 100 h were achieved with both structures. Since the initial resistance of the daisy-chain structures was dominated by that of the composite-based traces, and a higher rate of increase in resistance was observed with composites than sputtered Fe traces under degradation (shown in Fig. 4), the increased resistance exhibited by the daisy-chain structures under degradation should approximate the behavior of composite films under similar degradation conditions (i.e., both humid conditions), as demonstrated in Fig. 7. This suggested reasonable performance of the composites as interconnects during degradation. The stable electrical resistance of the micropatterned daisy-chain structures in biodegradable packaging supports the use of biodegradable composite-based interconnects for transient implantable applications.

IV. Application

Since the resistivity of the Fe-PCL composites is relatively high compared to nondegradable interconnect materials and increases as degradation proceeds, its effect on the power consumption and high-frequency signal transmission of potentially implantable electronic devices was explored. The maximum operational resistivity of the Fe-PCL composite

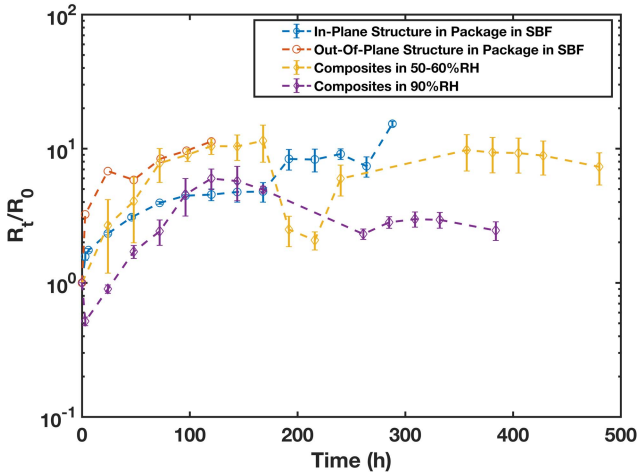

Fig. 7. Ratio of resistance change of packaged in-plane daisy-chain structure in SBF and Fe-PCL composite films degraded in humid conditions as a function of degradation time.

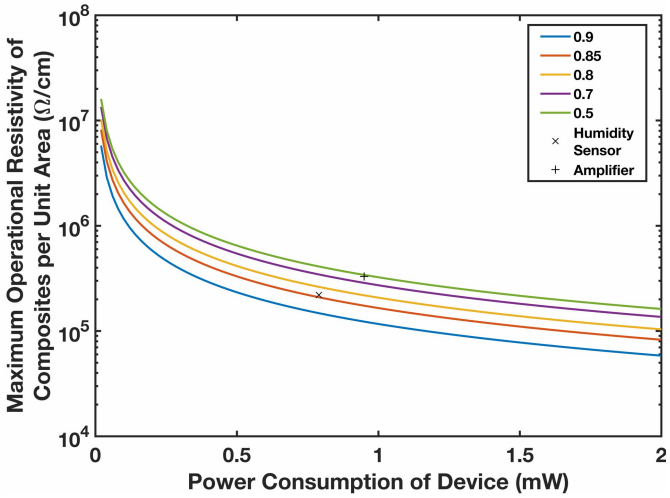

Fig. 8. Maximum operational resistivity of 0.1-mm-thick Fe-PCL biodegradable conductive polymer composites per unit area as a function of power consumption of the device, parameterized by the ratio of the device's voltage and supply voltage.

was analytically derived as a function of power consumption and the operating frequency of the device. Interestingly, the relatively high resistivity of the biodegradable composite compared with commercial, nonbiodegradable composite interconnect materials may not preclude its use in implant applications since many implantable devices intentionally operate at low voltages and frequencies compared with their external counterparts.

The calculations were experimentally confirmed using two circuit testbeds: a commercial humidity sensor (HDC1008) and a commercial differential amplifier (LM324-N), respectively. In the first testbed, a custom-programmed microcontroller provided the signal input to the humidity sensor. The sensor was powered by a power supply at 3.6 V. Resistors of various magnitudes were added to the power line to simulate the effect of the composite resistivity. The corresponding voltage across the sensor and current in the power line were measured. In addition, various resistances were added in series to the clock line (operating at 7.813 kHz). The corresponding clock signal was observed with an oscilloscope. A similar test setup was developed with the differential amplifier testbed.

First, the effect of the resistivity of the composites on the supply voltage is considered. Modeling the testbed by the series interconnection of a supply, a resistive composite, and a testbed device yields

$$V_{\text{supply}} = V_{\text{device}} + V_{\text{composites}}. \tag{1}$$

This can be written in terms of the device voltage and series current

$$\begin{aligned} V_{\text{device}} &= V_{\text{supply}} - V_{\text{composites}} \\ &= V_{\text{supply}} - I * R_{\text{composites}}. \end{aligned} \tag{2}$$

Writing (2) in terms of the power consumed by the device

$$V_{\text{device}} = V_{\text{supply}} - P_{\text{device}}/V_{\text{device}} * R_{\text{composites}}. \tag{3}$$

Rearranging for the resistance of the composite interconnect yields

$$R_{\text{composites}} = \left(V_{\text{supply}} * V_{\text{device}} - V_{\text{device}}^2\right)/P_{\text{device}}. \tag{4}$$

Equation (4) can be rewritten in terms of the areal resistivity of the composite interconnect

$$\begin{aligned} \rho_{\text{composites}}/A &= \frac{V_{\text{supply}} * V_{\text{device}} - V_{\text{device}}^2}{P_{\text{device}} * T_{\text{composites}}} \\ &= \frac{3.6 * V_{\text{device}} - V_{\text{device}}^2}{P_{\text{device}} * 0.01} \quad (\Omega/\text{cm}) \end{aligned} \tag{5}$$

where the second part of (5) assumes a supply voltage of 3.6 V and a typical interconnect thickness of 0.1 mm.

Equation (5), plotted as Fig. 8, shows the maximum operational resistivity of the Fe-PCL interconnect (0.1 mm thick) normalized by contact area as a function of device power consumption, parameterized by the ratio of device voltage to supply voltage. The humidity sensor retained functionality until the power supplied to it decreased to 0.79 mW at 3 V, which was observed with an Fe-PCL resistor of 2.2 kΩ. In turn, the amplifier operated functionally until the power supplied to it decreased to 0.95 mW at 1.8 V, observed with an Fe-PCL resistor of 3.3 kΩ. The results were consistent with analytical calculations (see Fig. 8). For example, if the contact area is 1 mm^2, the maximum supported resistivity of a 0.1-mm-thick composite interconnect in use with the humidity sensor testbed and the amplifier testbed is 2200 and 3300 Ω · cm, respectively. This approximated the maximum resistivity of packaged Fe-PCL composites degraded for over 400 h (see Fig. 4). Thus, test results support the use of Fe-PCL composites for interconnect applications, including routing to power sources.

In addition to the supply of dc power, lossy interconnect could potentially degrade device performance through an increased *RC* time constant on ac output lines. The relationship between the composite resistance and the operation frequency

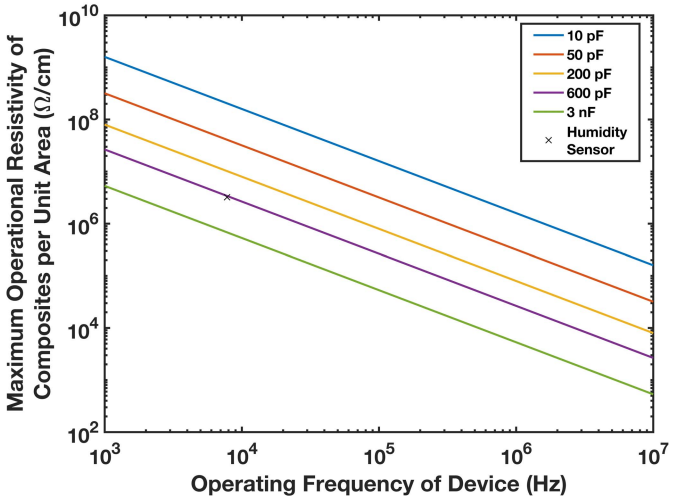

Fig. 9. Maximum operational resistivity of 0.1-mm-thick Fe-PCL biodegradable conductive polymer composites per unit area as a function of the operating frequency of the device, parameterized by input capacitance of the device.

can be estimated as

$$R_{\text{composites}} = 1/(2\pi f C_L) \tag{6}$$

where f is the cutoff frequency and C_L is the input capacitance of the device. Again, assuming the thickness of the composites is 0.1 mm

$$\begin{aligned}\rho_{\text{composites}}/A &= 1/(2\pi f C_L * T_{\text{composites}}) \\ &= 1/(2\pi f C_L * 0.01) \quad (\Omega/\text{cm}).\end{aligned} \tag{7}$$

Equation (7) is plotted in Fig. 9. It shows the maximum operational electrical resistivity of a 0.1-mm-thick Fe-PCL composite normalized by contact area as a function of operating frequency of the device, parameterized by the input capacitance of the device. In the humidity sensor testbed, the frequency of the clock line was 7.813 kHz and the input capacitance was 610 pF. The sensor responded to this frequency until the Fe-PCL interconnect resistance reached 32 kΩ. The result was consistent with our calculation (shown in Fig. 9). Assuming the contact area is 1 mm^2, the maximum supported resistivity of a 0.1-mm-thick composite in the aforementioned case is $3.2 \times 10^4 \Omega \cdot$ cm, which is larger than the maximum resistivity of packaged composites after 400 h of degradation (see Fig. 4). Thus, the test result highlighted the potential of Fe-PCL composite interconnects in applications in this frequency range.

V. Conclusion

In this study, the suitability of Fe-PCL composites as potential candidates for biodegradable electrical interconnects was investigated. In physiological degradation, the electrical percolation threshold of Fe-PCL composites was found to be 17%vf of Fe. The stability of resistivity over a reasonable functional lifetime was achieved by utilizing composites with 40%vf Fe, in excess of the percolation threshold. Short-term adhesion testing indicated reasonable adhesive stability of these interconnect materials. These properties suggest their potential application as interconnects. In emulated packaged degradation, an approximately tenfold increase in electrical resistivity of the composites was observed. The biodegradable electrical interconnects were shown to be compatible with standard processing techniques through the formation of micropatterned daisy-chain structures. Reasonable electrical stability of the daisy-chain structures in biodegradable packaging was demonstrated under physiological degradation, and system integration with commercial electronic components confirmed the feasibility of biodegradable Fe-PCL composites for interconnect applications in transient implantable systems.

References

[1] E. H. Ledet, D. D'lima, P. Westerhoff, J. A. Szivek, R. A. Wachs, and G. Bergmann, "Implantable sensor technology: From research to clinical practice," *J. Amer. Acad. Orthopaedic Surgeons*, vol. 20, no. 6, pp. 383–392, Jun. 2012.

[2] C. M. Boutry, H. Chandrahalim, P. Streit, M. Schinhammer, A. C. Hänzi, and C. Hierold, "Towards biodegradable wireless implants," *Philos. Trans. Roy. Soc. A, Math., Phys. Eng. Sci.*, vol. 370, no. 1967, pp. 2418–2432, May 2012.

[3] M. Luo, A. W. Martinez, C. Song, F. Herrault, and M. G. Allen, "A microfabricated wireless RF pressure sensor made completely of biodegradable materials," *J. Microelectromech. Syst.*, vol. 23, no. 1, pp. 4–13, Feb. 2014.

[4] T. Zhang, M. Tsang, and M. G. Allen, "Biodegradable electrical interconnects for transient implantable systems," in *Proc. 17th Hilton Head Workshop, Solid-State Sens., Actuators Microsyst.*, 2016, pp. 328–331.

[5] B. S. Klosterhoff *et al.*, "Implantable sensors for regenerative medicine," *J. Biomech. Eng.*, vol. 139, no. 2, Jan. 2017, Art. no. 021009.

[6] M. Luo, W. Shen, Y. Wang, and M. G. Allen, "*In vitro* degradation of biodegradable metal Zn and Zn/Fe-couples and their application as conductors in biodegradable sensors," in *Proc. 18th Int. Conf. Solid-State Sens., Actuators Microsyst. (TRANSDUCERS)*, Jun. 2015, pp. 1370–1373.

[7] L. Yin *et al.*, "Materials, designs, and operational characteristics for fully biodegradable primary batteries," *Adv. Mater.*, vol. 26, no. 23, pp. 3879–3884, Jun. 2014.

[8] M. Tsang, A. Armutlulu, A. W. Martinez, S. A. B. Allen, and M. G. Allen, "Biodegradable magnesium/iron batteries with polycaprolactone encapsulation: A microfabricated power source for transient implantable devices," *Microsyst. Nanoeng.*, vol. 1, Oct. 2015, Art. no. 15024.

[9] Y. Li and C. P. Wong, "Recent advances of conductive adhesives as a lead-free alternative in electronic packaging: Materials, processing, reliability and applications," *Mater. Sci. Eng., R, Rep.*, vol. 51, nos. 1–3, pp. 1–35, Jan. 2006.

[10] M. Vert, "Bioresorbable polymers for temporary therapeutic applications," *Die Angew. Makromolekulare Chem.*, vol. 166, no. 1, pp. 155–168, Feb. 1989.

[11] L. S. Nair and C. T. Laurencin, "Biodegradable polymers as biomaterials," *Prog. Polym. Sci.*, vol. 32, no. 8, pp. 762–798, Aug./Sep. 2007.

[12] P. A. Gunatillake and R. Adhikari, "Biodegradable synthetic polymers for tissue engineering," *Eur. Cell Mater.*, vol. 5, no. 1, pp. 1–16, May 2003.

[13] M. P. Staiger, A. M. Pietak, J. Huadmai, and G. Dias, "Magnesium and its alloys as orthopedic biomaterials: A review," *Biomaterials*, vol. 27, no. 9, pp. 1728–1734, Mar. 2006.

[14] H. Hermawan, D. Dubé, and D. Mantovani, "Developments in metallic biodegradable stents," *Acta Biomaterialia*, vol. 6, no. 5, pp. 1693–1697, May 2010.

[15] A. Bunde and W. Dieterich, "Percolation in composites," *J. Electroceramics*, vol. 5, no. 2, pp. 81–92, Oct. 2000.

[16] M. Weber and M. R. Kamal, "Estimation of the volume resistivity of electrically conductive composites," *Polym. Compos.*, vol. 18, no. 6, pp. 711–725, Dec. 1997.

[17] M. Peuster *et al.*, "A novel approach to temporary stenting: Degradable cardiovascular stents produced from corrodible metal—Results 6–18 months after implantation into new zealand white rabbits," *Heart*, vol. 86, no. 5, pp. 563–569, Nov. 2001.

[18] M. Peuster, C. Hesse, T. Schloo, C. Fink, P. Beerbaum, and C. V. Schnakenburg, "Long-term biocompatibility of a corrodible peripheral iron stent in the porcine descending aorta," *Biomaterials*, vol. 27, no. 28, pp. 4955–4962, Oct. 2006.
[19] H. Hermawan, A. Purnama, D. Dube, J. Couet, and D. Mantovani, "Fe–Mn alloys for metallic biodegradable stents: Degradation and cell viability studies," *Acta Biomater.*, vol. 6, no. 5, pp. 1852–1860, May 2010.
[20] L. Zhang, R. He, and H.-C. Gu, "Oleic acid coating on the monodisperse magnetite nanoparticles," *Appl. Surf. Sci.*, vol. 253, no. 5, pp. 2611–2617, Dec. 2006.
[21] J. Zhang, X. G. Chen, L. Huang, J. T. Han, and X. F. Zhang, "Self-assembled polymeric nanoparticles based on oleic acid-grafted chitosan oligosaccharide: Biocompatibility, protein adsorption and cellular uptake," *J. Mater. Sci., Mater. Med.*, vol. 23, no. 7, pp. 1775–1783, Jul. 2012.
[22] *Standard Test Methods for Measuring Adhesion by Tape Test*, Standard D. ASTM, 3359-09, American Society for Testing and Materials, 1998, pp. 1–7.
[23] E. Thommerel, J. C. Valmalette, J. Musso, S. Villain, J. R. Gavarri, and D. Spada, "Relations between microstructure, electrical percolation and corrosion in metal—Insulator composites," *Mater. Sci. Eng., A*, vol. 328, nos. 1–2, pp. 67–79, May 2002.
[24] J. Gakkestad, P. Dalsjo, H. Kristiansen, R. Johannessen, and M. M. V. Taklo, "Use of conductive adhesive for MEMS interconnection in ammunition fuze applications," *Proc. SPIE*, vol. 9, no. 4, Oct. 2010, Art. no. 041108.

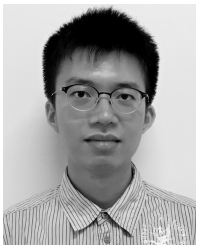

Tao Zhang received the B.E. degree in materials science and engineering from the South China University of Technology, Guangzhou, China, in 2013, and the M.S.E. degree in materials science and engineering from the University of Pennsylvania, Philadelphia, PA, USA, in 2015, where he is currently pursuing the Ph.D. degree in electrical engineering.

His current research interest includes the development and characterization of biodegradable electrical interconnects for transient implantable systems.

Melissa Tsang (S'14) received the B.S. degree in biomedical engineering from Brown University, Providence, RI, USA, in 2011, and the M.S. and Ph.D. degrees in electrical and computer engineering from the Georgia Institute of Technology, Atlanta, GA, USA.

Drawing upon her interdisciplinary training, she focused her graduate research on the development of microfabrication technologies for biodegradable materials and implementation of these approaches toward the design of MEMS-based biodegradable devices.

Dr. Tsang has been an NSF Graduate Research Fellow since 2011 and was a member of the MicroSensors and MicroActuators (MSMA) research group under the guidance of M. Allen.

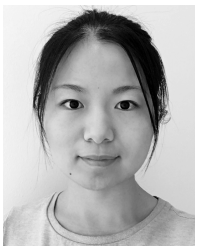

Lin Du received the B.S. degree in mechatronics engineering and the M.S. degree in mechanical engineering from the Beijing Institute of Technology, Beijing, China, in 2012 and 2015, respectively. She is currently pursuing the Ph.D. degree with the Department of Electrical and Systems Engineering, University of Pennsylvania, Philadelphia, PA, USA.

Her current research interest includes the implantable microelectromechanical system (MEMS) devices for human health monitoring systems with wireless transmission.

Minsoo Kim received the B.S. and M.S. degrees in electrical and computer engineering from Seoul National University, Seoul, South Korea, in 2006 and 2008, respectively, and the Ph.D. degree in electrical and computer engineering from the Georgia Institute of Technology, Atlanta, GA, USA, in 2016.

He is currently a Post-Doctoral Researcher with the Department of Electrical and Systems Engineering, University of Pennsylvania, Philadelphia, PA, USA. His current research interests include the development of electrodeposition-based technologies for the realization micro/nanohierarchical structures that lead to a variety of useful applications (e.g., nanoscale magnetic laminations for miniaturized dc–dc converters, drag reduced microfluidics, and nonlithographic nanopatterning).

Mark G. Allen (M'88–SM'04–F'11) received the B.A. degree in chemistry, the B.S.E. degree in chemical engineering, and the B.S.E. degree in electrical engineering from the University of Pennsylvania, Philadelphia, PA, USA, and the S.M. and Ph.D. degrees from the Massachusetts Institute of Technology, Cambridge, MA, USA, in 1989.

In 1989, he joined as a Faculty Member with the School of Electrical and Computer Engineering, Georgia Institute of Technology, Atlanta, GA, USA, ultimately holding the rank of Regents' Professor and the J. M. Pettit Professorship in Microelectronics, as well as a joint appointment with the School of Chemical and Biomolecular Engineering. In 2013, he left Georgia Tech to become the Alfred Fitler Moore Professor of Electrical and Systems Engineering and the Scientific Director of the Singh Nanotechnology Center, University of Pennsylvania. His current research interests include the development and the application of new micro and nanofabrication technologies, and MEMS.

Dr. Allen was the Editor-in-Chief of the *Journal of Micromechanics and Microengineering* and the Co-Chair of the IEEE/ASME MEMS Conference.